Original Research Article

Effect of sodium dodecyl sulphate (SDS) and electrochemical behavior of electrodeposited lead dioxide on nickel substrate for lead acid battery application

ABSTRACT

An investigation has been made to electrodeposit PbO_2 anodically by galvanostatic deposition method on Ni and Ag coated Ni substrate from highly alkaline lead acetate bath (0.2 M $CH_3(COO)_2$ and 5 M NaOH) in the presence of an anionic surfactant sodium dodecyl sulfate (SDS) for the application of lead-acid battery positive electrode. The electrodeposited PbO_2 was characterized sequentially by current efficiency and thickness measurement, visual and optical microscopic observation, cyclic voltammetry (CV) study, scanning electron microscopic (SEM), and X-ray diffraction (XRD) test. The results revealed that with the increase of SDS concentration the current efficiency as well as the thickness of PbO_2 deposits increased up to 100 mgL^{-1} SDS and afterward it decreased. The morphological study showed that PbO_2 particle size and morphology can be controlled by varying the concentration of SDS. The electrochemical behavior of the prepared samples in 4.7 M H_2SO_4 solution (lead-acid battery electrolyte concentration) was investigated using cyclic voltammetry. In the absence of SDS, a pure α PbO_2 relatively less stable (lasting up to 100 cycles), and larger-grained deposit with low charge-discharge density was formed. The addition of a small amount of SDS to the electrolyte increased the grain refinement of α-PbO_2 with compact and small-grained crystals, improving the stability (up to 350 cycles) and charge-discharge density of the PbO_2 film in the battery environment.

Keywords: *Electrodeposition; alpha-lead dioxide; nickel substrate, lead-acid battery, SEM, XRD*

1. INTRODUCTION

Electrical energy is one of the most widely used types of energy in the world. It is easily converted into any other form of energy and can be transported safely and efficiently over long distances. It is widely applicable and easily converted into light, heat, or mechanical energy. However, one general problem is that electrical energy is difficult to store. Capacitors enable direct storage, but the quantities available are small in comparison to the demand for most applications. Secondary storage batteries

are the best solution in this situation. Secondary batteries include lead-acid, nickel-cadmium, nickel-metal hydride, and lithium-ion batteries, as well as others. Among them, the lead-acid battery is the most commonly used rechargeable battery, with lead dioxide (PbO_2) pasted on a Pb grid serving as the positive electrode and metallic spongy lead with a high surface area serving as the negative electrode in a sulfuric acid electrolyte [1-3]. Due to their versatility, high reliability, high discharge rate, flexible performance, and ease of recycling, lead-acid batteries remain the most dominant electrical energy storage system nearly 150 years after their invention [4, 5]. In LAB spongy lead-coated lead and PbO_2 coated Pb is used as negative and positive electrode. Although lead-acid batteries are the most commonly used rechargeable battery system, this promising technology has some drawbacks that limit its application. The most significant disadvantage is its low energy density or specific energy per unit weight(30-40 $Whkg^{-1}$) [1]. Grid typically materials for both anode and cathode are lead or lead alloys, and due to their high density, grids carry a significant portion of the battery weight. This is the primary reason for lead-acid batteries' low specific energy per unit weight. The use of lightweight substrates instead of a Pb grid ~~will be a~~ promising solution for that. A lot of research on lightweight substrates Ti, [6, 7] boron-doped diamond (BDD) [8,9] glassy carbon electrode [10], Cu [11], platinum and Ni [12], gold [13] were used for electrodeposition of lead dioxide. Yolshina et al.[14] discovered that lead-covered copper grids as positive electrodes provide high discharge current density after depositing a lead film on copper and copper coated titanium substrates. Later, foam-based lead alloy positive electrodes were electrodeposited on a copper foam substrate to address the issues of high internal resistance and limited utilization of positive active materials (PAM) in lead-acid batteries [15]. The thickness of the lead coating had a significant impact on the corrosion resistance of the copper foam substrate. Furthermore, when compared to the cast grid battery, the lead-foam collectors improved the charge-discharge performance as well as the utilization efficiency of the PAM by 19–36 percent. PbO_2 crystals exist in two polymorphs: orthorhombic α-PbO_2 and tetragonal β-PbO_2, and their abundance is determined by deposition conditions and type of substrate [16]. In general, α -PbO_2 obtained from an alkaline solution with a more compact structure has better particle contact than β-PbO_2 which is obtained from an acidic medium. However, in dilute H_2SO_4 β-PbO_2 has superior catalytic activity [17, 18].

Cao et al. [19] prepared single-crystalline PbO_2 nanorods using a basic solution containing $Pb(NO_3)_2$ and cetyltrimethylammonium bromide (CTAB). Xi et al. [20] prepared sub-micrometer-sized PbO_2

Comment [C1]: Give in full at first appearanceand you use it subsequently

Comment [C2]: Seems to be

hollow spheres of about 200-400 nm from a basic solution of $Pb(NO_3)_2$ in the presence of PVP. In our previous work [21] we prepared an electrodeposited PbO_2 electrode on the Ni substrate from acidic lead nitrate medium in the presence of SDS and NaF and discovered that the presence of NaF and SDS in the depositing bath facilitated in grain refinement of the deposit. We found that Compact and small-grained deposits with a higher proportion of β -PbO_2 were formed, and they lasted for 300 cycles with a relatively higher charge-discharge density in 4.7 mol L^{-1} H_2SO_4 (battery electrolyte condition). In this work, we prepared an electrodeposited PbO_2 on Ni substrate from a basic lead acetate medium in the presence of SDS as surfactant and investigate its effect on the morphology, crystallinity, and electrochemical properties of prepared lead dioxide.

Comment [C3]: same

Comment [C4]: same

2. EXPERIMENTAL

2.1 Substrate

Commercially pure (99.9%) nickel sheets having a thickness of 0.5 mm cut into 1 cm × 4 cm coupons ~~were~~ used ~~as~~ substrate~~s~~ for the electrodeposition of PbO_2. Coupons were successively polished with SiC paper up to 1200 grit, washed with liquid soap solution, and immersed for 5 min in an aqueous 1% NaOH solution. After that, they were cleaned with distilled water and dried in the open air. Both sides of the coupons were painted with insulating paint leaving 1 cm^2 space exposed at one end for experiment. A small portion at the other end were also left bare for electrical contact. The coupons were then dried in an oven at 80°C for 1 hour for curing and removal of moisture. The coupons were weighted properly with an analytical balance after cooling it to room temperature and stored in a desiccator containing silica gel for the subsequent experiment.

Comment [C5]: was

Comment [C6]: a

Comment [C7]:

2.2 Solutions

Just before running any electrodeposition experiment, the prepared Ni coupon was dipped into 0.1 M H_2SO_4 for 10 minutes for surface activation. The reagents used in this study included lead acetate (Qualikems, India), sulfuric acid (BDH, England), sodium hydroxide (E. Merck, India), sodium dodecyl sulfate (Loba Chemie, India), The $Pb(CH_3COO)_2$ concentrations used in this study were 0.2 M, NaOH 5 M and SDS concentrations range from 10 mgL^{-1} to 500 mg L^{-1} respectively.

2.3 Electrodeposition of PbO_2

Using a precision-controlled regulated DC Power Source, PbO_2 has electrodeposited Galvano static mode by using a DC Power supply (Model PS 303, Loadstar Electronics, Taiwan). A 250 mL Pyrex glass beaker with 200 mL electrolyte was put on a temperature sensor hot plate with a magnetic stirring facility as the electrolytic cell (Model; MS300HS, Brand: Mtops Korea). Before and after each deposition the solution pH was ~~measured~~. The prepared Ni coupon connected to the positive terminal of the power source and another clean coupon connected to the negative terminal was placed in parallel 2 cm apart in the cell solution in such a way that the exposed surface was well immersed in the electrolyte, and the crocodile clips for electrical contact were well connected. For measuring current, a digital multimeter with zero resistance ammeter (Model 300D, Sanwa, digital multimeter, China) was connected in series. Pb^{2+} ions were oxidized and deposited on the anode as PbO_2 when a controlled current was applied. ~~Pb^{2+} ions were oxidized and deposited on the anode as PbO_2 when a controlled current was applied.~~ The anode was carefully cleaned with distilled water and dried in an oven for one hour at 80°C after electrodeposition for the recommended condition, and the weight was then measured correctly at room temperature. The difference in the weight of the coupon after and before electrodeposition determined the amount of PbO_2 deposited. Using faraday's law of electrolysis, the current efficiency and thickness of the deposition were calculated. ~~The amount of PbO_2 deposited was the difference in the weight of the coupon after and before electrodeposition. The deposition current efficiency and thickness were calculated by using faraday's law of electrolysis.~~ Each experiment was repeated at least three times to check the reproducibility.

Comment [C8]: sentence not clear

Comment [C9]: determined

2.4 Morphology and crystal structure determinations

Surface microstructure characterization was carried out by using a high-resolution Optical Microscope (OM) (ACME 40x-640x Digital Metallurgical Microscope, India) and Scanning Electron Microscope (SEM) (FEI Inspect S50, Oregon, USA). The coated samples were sputtered with a conductive coating (gold) before taking images. To undergo XRD analysis, the PbO_2 deposits were washed with acetone, dried, detached from the substrate, and ground in a mortar. Then the powder was compressed on glass for diffraction. X-ray diffraction analysis was performed using a Philips X'pret MPD diffractometer with a Cu Kα radiation (λ = 1.5418 Å); generator settings: 40 kV, 30 mA; step size: 0.02°; and 2θ range: 20°-80°C.

2.5 Cyclic voltammetry characterization

The cyclic voltammetry experiment was carried out in a three-electrode cell arrangement with deposited PbO2 as a working electrode (WE), SSE with Luggin capillary probe as a reference electrode, and Pt wire gauge as a counter electrode on a Gill AC Impedance Analyzer (ACM Instruments, England). All voltammetry experiments were performed under static conditions in 4.7 M H_2SO_4 at 30°C. The charge and discharge densities were calculated by dividing the area under the peak or peak position by the scan rate, and the discharge efficiency was calculated by dividing the discharge density by the charge density.

Comment [C10]: check

3. RESULTS AND DISCUSSION

3.1 Electrolysis

Fig.1 shows the current efficiency (CE) and thickness of electrodeposited PbO_2 prepared with and without anionic surfactants SDS. The surfactant-free bath yields PbO_2 with a CE of 96 percent and thickness of 45.1 µm. when the surfactant is added, the CE increases to a maximum (marked as optimum surfactant concentration) (for anionic surfactant SDS) before decreasing with the addition of excess surfactant. In presence of SDS, the oxygen evolution decreases thus the CE increases. [22]. But at a high concentration of SDS the current efficiency and thickness decrease due to the blocking effect.

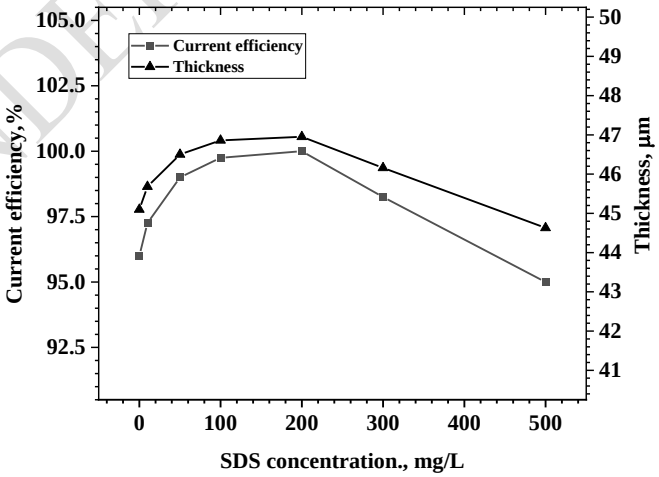

Fig.1 Current efficiency and thickness of PbO_2 films prepared at constant current densities of 10 mA cm^{-2} for 60 min.

From the Fig.1, it is clear that with increasing SDS concentration current efficiency and thickness increase up to 200 mg/L afterward decreasing the CE and thickness.

Comment [C11]: increased

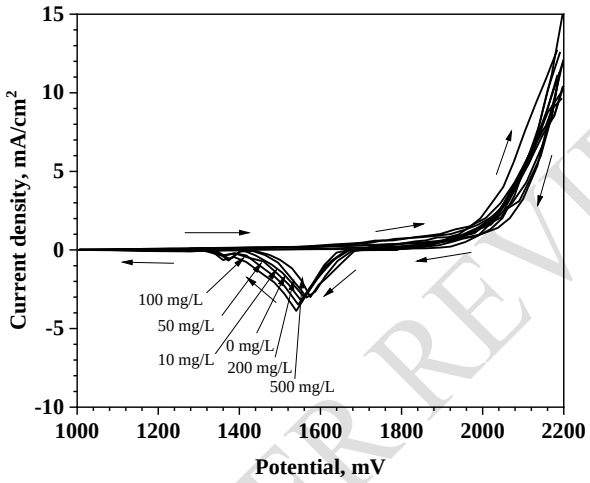

Fig. 2 Cyclic voltammograms of PbO_2 films prepared at constant current densities of 10 mA cm^{-2} for 90 min at 55° C from the solution containing 0.2 M lead acetate and 5 m NaOH in the presence of 0.10, 50, 100, 200, and 500 mg/L SDS. The cyclic voltammetry was carried out in a 4.7 M H_2SO_4 solution at a 30 mV/s scan rate maintaining at 30 °C.

Fig.2 shows cyclic voltammograms of PbO_2 in 4.7 M H_2SO_4. The voltammograms were started anodically at 1000 mV at a scan rate of 30 mV/s and extended up to 2200 mV. The potential was measured concerning saturated Ag/AgCl electrodes (SSE). The PbO_2 was electrodeposited on the Ni-substrate from a solution containing 0.2 M $Pb(CH_3COO)_2$ in 5 M aqueous NaOH at 55^0C temperature using 10 mA/cm^2 current density in presence of 0, 10, 50, 100, 200, and 500 mg/L SDS. As shown in the figure, during the anodic scan of all the PbO_2 electrodes a steady current rise was observed after 2000 mV without the appearance of any peak. As PbO_2 was already electrodeposited on the electrode, the current was mainly due to oxygen evolution reaction [23-26]. During the reverse sweep, two well-defined peaks were observed due to the reduction of PbO_2 to $PbSO_4$ at around 1560 mV and 1430 mV for PbO_2 obtained from 50, 100 mg/L SDS containing solution and other PbO_2 electrode

show only one peak for the conversion of α PbO_2 to $PbSO_4$. However, it could be seen that the reduction potential shifted more negative direction with increasing of SDS concentration up to 100 mg/L but decreased at 200mg and 500 mg/L SDS concentration. In addition, the amount of charge involved during PbO_2 reduction using the electrode constructed at an SDS concentration of 100 mg/L appeared to be the highest of the six samples. This suggests that the PbO_2 electrode with an SDS concentration of 100 mg/L can have more active materials involved in the sulfuric acid discharge cycles. Since, the SEM and XRD results revealed this, 100 mg/L SDS was used as the optimum condition for my experiment.

3.2 Cyclic voltammetry/Charge discharge cycle life

A porous structure is conducive to improving the utilization of PbO_2 active materials; however, excessive porosity reduces particle connectivity, reducing the discharge capacity of the active materials significantly [27]. The CV results, clearly show that the micro/nano-structured PbO_2 thin films made of small nanoparticles exhibit high electrochemical performance. We compared the charge/discharge cycling life of three typical PbO_2 thin films that were electrochemically prepared at 0 mg/L SDS, 100 mg/L SDS and 100 mg/L SDS on silver-coated Ni respectively, and further characterized the microstructure and morphology of that thin-film materials by SEM, Optical Microscopic Examination and XRD to confirm the viewpoint [28]. Cyclic voltammetry provides more information about electrochemical reaction mechanisms, stability, performance, and side reaction conditions. All cyclic voltammetry experiments were performed in 4.7 mol /L H_2SO_4 acid (approximate concentration of H_2SO_4 in the lead-acid battery) at room temperature and potential between 1000 and 2200 mV at 30 mV/S scan rate to better understand the phenomena occurring in lead-acid battery conditions.

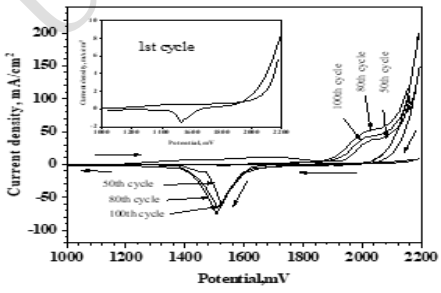

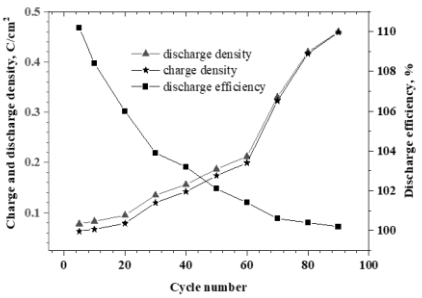

Fig. 3 (a) Cyclic voltammetry and (b) Charge-discharge current density and discharge efficiency of PbO_2 in 4.7 M H_2SO_4 at 30 °C. PbO_2 film was electrodeposited from a solution containing 0.2 M $Pb(CH_3COO)_2$ and 5 M NaOH at 10 mA /cm^2 current density and 55°C for 90 min.

Fig. 3 (a) shows a cyclic voltammogram of electrodeposited PbO_2 in 4.7M H_2SO_4. The voltammograms were started anodically at 1000 mV at a scan rate of 30 mV/s and extended up to 2200 mV. The potential was measured with respect to saturated Ag/AgCl electrodes (SSE). The PbO_2 was electrodeposited on the Ni-substrate from a solution containing 0.2 M $Pb(CH_3COO)_2$ in 5 M aqueous NaOH at 55^0C temperature using 10 mA/cm^2 current density in absence of SDS additives. Before running successive cycles, open circuit potential (OCP) was noted up to the stable which was 1556 mV. The oxidation of PbO to Pb_3O_4 ($2PbO.PbO_2$) (up to 1200 mV) [29] and Pb_3O_4 to PbO_2 Pb_3O_4 to PbO_2 [16] may result in a small amount of current (~0.2 mA /cm^2) in the potential range between 1000 mV and 1850 mV (beginning of O_2 evolution) during the anodic scan of the first cycle (elaborated in the inset). After 2000 mV current started to rise sharply due to oxygen evolution reaction [23-26]. During the cathodic scan of the 1st cycle, two well-defined small peaks at 1560 mV and 1430 mV were reduced of PbO_2 to $PbSO_4$ [16]. PbO_2 can exist as α-PbO_2 (orthorhombic structure) and β-PbO_2 (tetragonal structure), and their relative amounts of deposition during PbO_2 formation depend on the pH of the electrolytic medium and other factors as reported in the literature [16, 30]. According to the literature reports [11, 31] mixtures of α- and β-PbO_2 electrodeposit from acidic medium, but in alkaline medium only α-PbO_2 forms [32]. It has been reported [33] that reduction of α-PbO_2 to $PbSO_4$ takes place at relatively more positive potential compared to that of β-PbO_2. So, in the cathodic scan of all cases, peaks at more positive potential were due to the reduction of α-PbO_2, and less positive potential was due to the reduction of β-PbO_2 to $PbSO_4$ respectively [34]. In the present work electrodeposition of PbO_2 was carried out in alkaline media, so deposit was mainly α-PbO_2. However, cyclic voltammetry was carried out in a highly acidic medium (4.7M H_2SO_4), so there might be the instantaneous conversion of some pure α-PbO_2 to β-PbO_2. The 50^{th} cycle shows the anodic peak current of 38 mA/cm^2 at around 2004 mV for the conversion of $PbSO_4$ to PbO_2 which merged with oxygen evolution reaction (OER) after 2140 mV [21]. During the cathodic scan two peaks at 1526 mV and 1446 mV with peak current densities of 62 mA/cm^2 and 10 mA/cm^2 were due to the conversion of α-PbO_2 to $PbSO_4$ and β-PbO_2 to $PbSO_4$ respectively [34]. The 80^{th}

cycle of anodic scan shows a peak at the same position as the 50th cycle but with a higher current density (48 mA/cm^2) due to $PbSO_4$ conversion to PbO_2. The corresponding cathodic sweep demonstrates cathodic peaks shifted to negative potential than 50th cycle at 1507 mV with a peak current density of 75 mA/cm^2 and β-PbO_2 merge with α-PbO_2. As the cyclic voltammogram is carried out in an acidic medium (4.7M H_2SO_4) $PbSO_4$ is mainly oxidized to β-PbO_2. So, with increasing cycle number amount of β-PbO_2 also increases on the surface of the electrode. So, there is always a mixture of α-PbO_2 and β-PbO_2 present on the surface. That is why with increasing cycle number PbO_2 to $PbSO_4$ conversion peak shifts to the negative direction in Fig.3(a) [35]. Both the anodic and cathodic peak current densities were lower in the case 100th cycle than in the 80th cycle and a broad and swallow peak between 1420-1800 mV was found due to the oxidation of Ni to NiO(OH) [21,36, 37]. Fig. 3b shows the effect of cycling on charge ($PbSO_4$ to PbO_2) and discharge (PbO_2 to $PbSO_4$) current densities. The graph shows that the charge and discharge current densities increase steadily with cycle number until the 80th cycle, when they became constant. Because the surface was entirely composed of PbO_2 film at the start of the charging cycle, no conversion of $PbSO_4$ to PbO_2 occurred. However, $PbSO_4$ was formed from PbO_2 during the subsequent discharge cycle. As a result, the charge density was lower than the corresponding discharge density at the start of the CV. As the cycling progressed, a more porous PbO_2 film with a larger surface area formed, allowing H^+, HSO_4^-, and H_2SO4 to interact with the active material. As a result, both the charge and discharge densities increased [35]. Also through the more porous structure Ni come in contact with H_2SO_4, corroded and goes to solution. As a result the PbO_2 electrode become damaged. α -PbO_2, β -PbO_2, and $PbSO_4$ have densities of 9.87 g /cm^3, 9.3 g /cm^3, and 6.29 g /cm^3, respectively [38]. During successive cycling due to volume expansion and contraction a stress developed on the PbO_2 which is responsible for parting away from the substrate at higher cycles in H_2SO_4. The initial discharge efficiency above 110 percent significantly dropped as the cycle number increased. This means that when no $PbSO_4$ was present, the initial discharge (PbO_2 to $PbSO_4$) current density of the PbO_2 film was greater than the corresponding charge ($PbSO_4$ to PbO_2) current density. Because of the increased oxygen evolution from the active surface, discharge efficiency decreased as the cycle number increased. The abundant oxygen evolution in the latter stages of cycling merged with the charge current density, which contributes to a decrease in discharge efficiency. This implies that the surface area of the PbO_2

film was reduced as a result of a significant amount of PbO_2 falling apart from the Ni substrate. OCP drops to 235 mV after the 100th cycle.

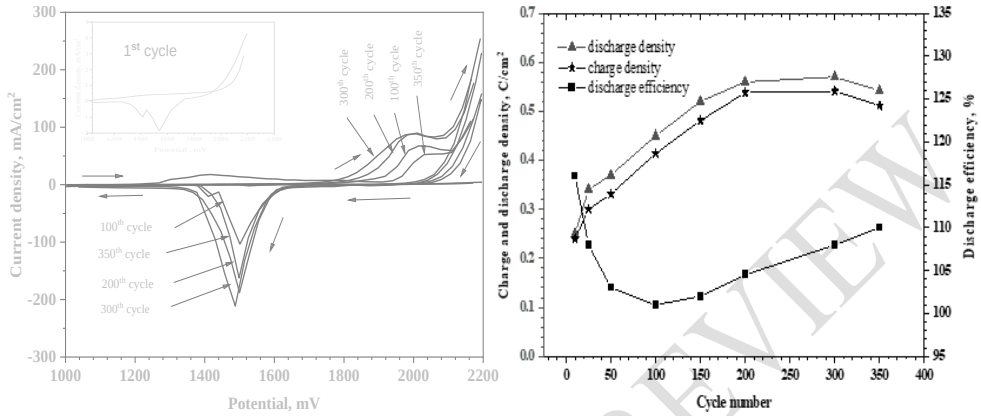

Fig. 4 (a) Cyclic Voltammogram and (b) Charge-discharge current density and discharge efficiency for PbO_2 Electrodeposited from the plating bath of Fig. 3 with an additional 100 mg/ L SDS in the solution

Fig. 4(a) Shows the results of a cyclic voltammogram obtained from a PbO_2 film deposited on a Ni substrate under the same conditions as in Fig. 3 (a). but with an additional 100 mg/L SDS in the electrolyte. Cyclic voltammetry condition was also the same as Fig. 3 (a) The cyclic voltammetry was continued up to 350 cycles. Afterward, it was discontinued due to the rapid deterioration of the deposited surface. Before starting successive cycle open circuit potential (OCP) was recorded to be stable which was 1560 mV. OCP dramatically dropped after the 350th cycle The voltammogram for 1st, 100th, 200th, 300th and 350th cycles are shown in Fig.4(a) All have distinct anodic and cathodic peaks with higher current densities when compared to Fig. 3(a), the corresponding cycles when deposited on Ni substrate. Each case Peak shifted to more negative potential and peak current also increased up to 300 cycles. After 350 cycles both anodic and cathodic peak current decreased and Ni oxidation current was found and Ni goes to the solution. After the 350 cycles, the open circuit potential decreased to 280 mV as the nickel surface was exposed to the sulfuric acid solution. In H_2SO_4 media, the 300th cycle was completed without any nickel corrosion. This indicates that the nickel surface has completely covered with the PbO_2 film. PbO_2 could not protect base nickel from corrosion even after 60 cycles in the absence of SDS (Fig. 3a), whereas with additive (SDS), the protection limit was

above 350 cycles. Surprisingly, no anodic current for nickel oxidation up to 350 cycles, indicating the surface's remarkable stability. The charge and discharge behavior is as usual as the above-mentioned Fig.3 (b).

3.3. Correlation of electrochemical properties with surface microstructure

Optical Microscopic Examination and Scanning Electron microscopic Examination (SEM) were used to examine the size and morphology of the synthesized films.

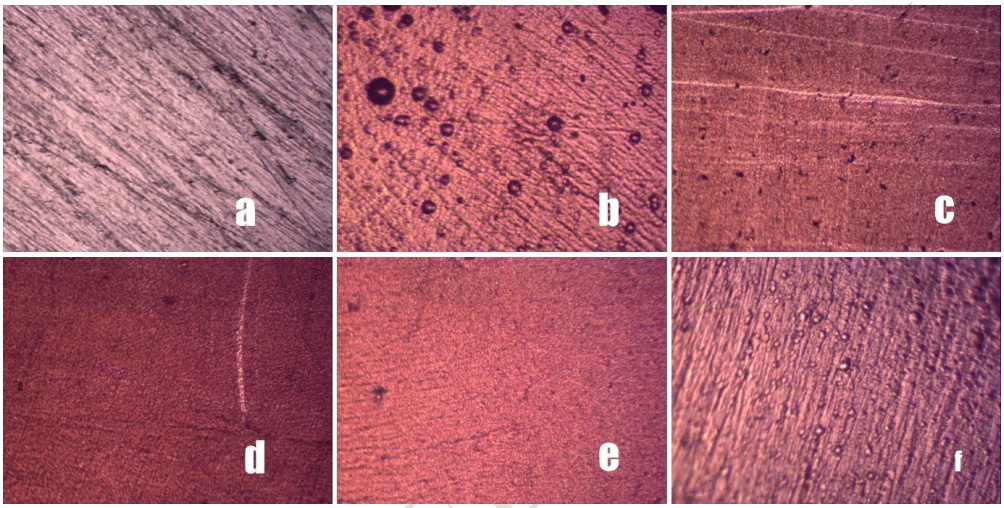

Fig.5 Optical Microscopic picture of electrodeposited PbO_2 from 0.2M $Pb(CH_3COO)_2$ solution in 5 M NaOH. The deposition current density was 10 mA/cm^2 for constant 36 coulombs of electricity at 55°C (a) Pure Ni sheet (b)in absence of SDS (c) in presence of 50 mg/L SDS (d) in presence of 100 mg/L SDS (e) in presence of 200 mg/L SDS (f) in presence of 500 mg/L SDS. Magnification was10X × 40X.

Fig.5 shows the Optical Microscopic Examination of the electrodeposited PbO_2. From the microscopic figure, it is clear that in the absence of SDS (Fig. 6(b) non uniform and larger particle-sized agglomerated particles with holes and pores are present on the surface. With increasing the concentration of the SDS amount of agglomerated particles and holes is decreased. At 100 and 200 mg/L SDS concentration uniformly deposited non-agglomerated particles are found. At 500 mg/L SDS, the agglomerated particles coalesce into aggregated PbO_2 particles and more compact deposits are formed. All of these are also supported by SEM, XRD, and Cyclic voltammetry (CV) experiments.

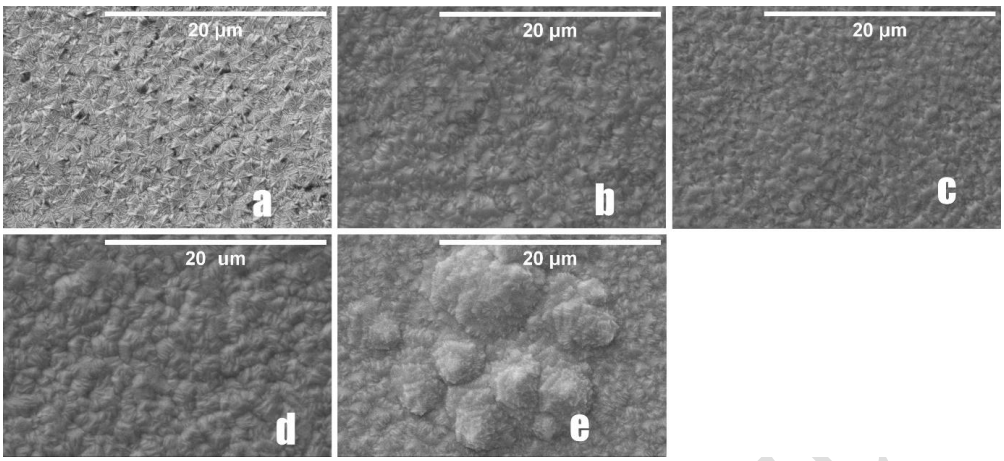

Fig.6 Scanning Electron Microscopic (SEM) picture of electrodeposited PbO2 from 0.2M $Pb(CH_3COO)_2$ solution in 5 M NaOH. The deposition current density was 10 mA/cm^2 for constant 36 coulombs of electricity at 55℃ (a) in absence of SDS (b) in presence of 50 mg/L SDS (c) in presence of 100 mg/L SDS (d) in presence of 200 mg/L SDS (e) in presence of 500 mg/L SDS. Magnification was 10000×.

From Fig. 6, it can be found the SDS concentration affects the morphology of electrodeposited PbO_2. PbO_2 prepared in the absence of SDS are noticeably larger (microstructures) than those prepared with the surfactant SDS (nanostructures). The sample with no SDS consists of larger-sized flower-like particles of the highest and lowest particle range is 3 µm - 542 nm (Fig. 6a), which are themselves composed of smaller non-uniform rod-like crystallites of the biggest grain with 163 nm long and 15 nm wide, and the smallest one with 41 nm long and 6 nm wide (Fig.6b) with several holes and pores. In the presence of SDS more compact and decreased particle-sized PbO_2 was obtained. The PbO_2 at 50 mg/L SDS (Fig. 2b) consists of flower-like particles of the highest and lowest particle range is 1.8 µm - 272nm composed with a relatively smaller sized rod-like particles of the biggest grain with 33 nm long and 6 nm wide, and the smallest one with 16 nm long and 6 nm wide (Fig.6 b) with less pore and holes. In the case of 100 mg/L SDS, PbO_2 particles are composed of smaller flower-like grain in the range of (1.2 µm - 240 nm) comprise of (16-28) nm length and 6 nm wide particles (Fig.6c). For 200 mg/L SDS containing PbO_2 sample consists of (28-12) nm length and 6 nm wide. In the case of 500 mg/L, SDS containing PbO_2 the smaller sized particles (1 µm – 240) nm particles comprised with (16-28) nm length and 6 nm wide particles coalescence and form aggregates of PbO_2 particles of (5-34)

μm. The presence of SDS made the PbO_2 surface smoother and more adherent to the substrate, resulting in better performance during cycling in H_2SO_4 . Because the thicknesses of the two deposits (in the absence and presence of SDS) were nearly identical (79 um), the PbO_2 film deposited from the SDS-containing solution was expected to have more layers from the one deposited in the absence of SDS because the latter had a larger grain size. As a result, electrolytes such as H^+ and HSO_4^- are less capable of penetrating the PbO_2 film deposited in the presence of SDS during the $PbSO_4$ to PbO_2 to $PbSO_4$ conversion process and exhibit maximum stability in H_2SO_4, as previously observed in cyclic voltammetry experiments (Fig. 3a and Fig. 4a).

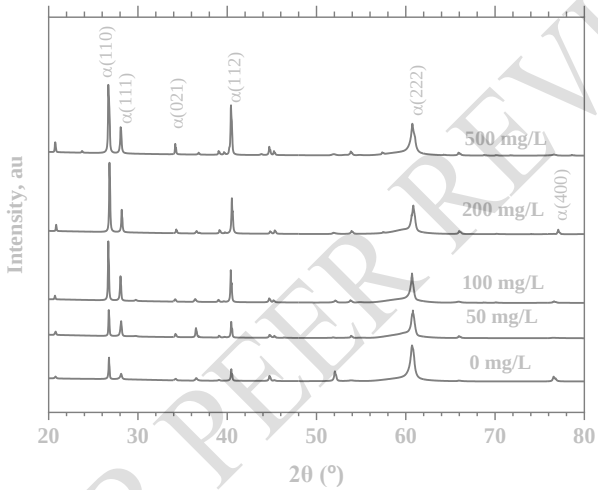

Fig.7 X-ray diffractograms of PbO_2 electrodeposited on Ni-substrate from an electrolyte containing 0.2M lead acetate in 5M NaOH at 10 mA/cm^2 current density for the thickness of 74 um for all cases at 55^{o}C at different concentrations of SDS.

The phase composition of electrodeposited PbO_2 samples was determined using X-ray diffraction. Generally, PbO_2 can be found in two forms: tetragonal β - PbO_2 and orthorhombic α-PbO_2. The structure of α -PbO_2 is more compact than that of more porous β -PbO_2, resulting in better particle contact.

Fig.7 shows the XRD graph of electrodeposited PbO_2 on Ni substrate electrodeposited from a solution of 0.2 M $Pb(CH_3COO)_2$ and 5 M NaOH containing 0, 50, 100, 200, and 500 mg/L SDS on Ni substrate. Only the characteristic peaks of α - PbO_2, denoted by the Miller number, have been observed for all the deposited samples, as shown in Fig. 7. According to previous research, lead

dioxide electrodeposited from acidic Pb^{2+}solution exists in the form β-PbO_2, but in alkaline solution, α-PbO_2 is the dominant form [39, 40]. 500 mg/L SDS shows a higher degree of crystallinity while 0 mg/L SDS containing electrode shows a lower degree of crystallinity.

4. Conclusions

PbO_2 film was deposited on the Ni substrate using galvanostatic anodic deposition from alkaline $Pb(CH_3COO)_2$ in the presence of SDS additive for use as a positive electrode in a lightweight lead-acid battery.

The following are the findings of the study:

- SDS concentration had a much stronger influence on the surface morphology. It has been shown that lead dioxide electrodeposited from 100 mg/L SDS on bare Ni and Ag coated Ni had more uniform nanocrystals.
- From the XRD data, it was seen that the presence of SDS increased the α PbO_2.into the PbO_2 electrode.
- From the cyclic voltammetry studies, it was found that the higher oxygen evolution potential and lower oxygen evolution peak current were obtained for 100 mg/L SDS-containing electrodes. And also increased number of the charged discharged cycle was obtained for 100 mg/L SDS on Ni. In the case of 100 mg/L SDS addition in the electrolyte solution, the stability became 4.5 times higher than 0 mg/L SDS.

COMPETING INTERESTS DISCLAIMER

Authors have declared that no competing interests exist. The products used for this research are commonly and predominantly use products in our area of research and country. There is absolutely no conflict of interest between the authors and producers of the products because we do not intend to use these products as an avenue for any litigation but for the advancement of knowledge. Also, the research was not funded by the producing company rather it was funded by personal efforts of the authors.

References

[1] T. B. R. D. Linden, *Handbook of Batteries*, 3rd ed. McGraw-Hill, 2001.

[2] D. Pavlov, *Lead Acid Batteries; Science and Technology*. Elsevier, Amsterdam, 2011.

[3] B. Rezaei and M. Taki, “Effects of tetrabutylammonium hydrogen sulfate as an electrolyte additive on the electrochemical behavior of lead acid battery,” pp. 1663–1671, 2008, doi: 10.1007/s10008-008-0547-x.

[4] R. Inguanta, S. Piazza, and C. Sunseri, “Growth and Characterization of Ordered PbO[sub 2] Nanowire Arrays,” *J. Electrochem. Soc.*, vol. 155, no. 12, p. K205, 2008, doi: 10.1149/1.2988728.

[5] L. Zhao *et al.*, “Aqueous batteries as grid scale energy storage solutions,” *Renew. Sustain. Energy Rev.*, vol. 68, no. 1, pp. 1174–1182, 2017, doi: 10.1016/j.rser.2016.02.024.

[6] Y. Mohd and D. Pletcher, “The fabrication of lead dioxide layers on a titanium substrate,” *Electrochim. Acta*, vol. 52, no. 3, pp. 786–793, 2006, doi: 10.1016/j.electacta.2006.06.013.

[7] J. Lee, H. Varela, S. Uhm, and Y. Tak, “Electrodeposition of PbO2 onto Au and Ti substrates,” *Electrochem. commun.*, vol. 2, no. 9, pp. 646–652, 2000, doi: 10.1016/S1388-2481(00)00095-3.

[8] A. J. Saterlay, S. J. Wilkins, K. B. Holt, J. S. Foord, R. G. Compton, and F. Marken, “Lead Dioxide Deposition and Electrocatalysis at Highly Boron-Doped Diamond Electrodes in the Presence of Ultrasound,” pp. 66–72, 2001, doi: 10.1149/1.339874.

[9] V. Suryanarayanan, I. Nakazawa, S. Yoshihara, and T. Shirakashi, “The influence of electrolyte media on the deposition/dissolution of lead dioxide on boron-doped diamond electrode - A surface morphologic study,” *J. Electroanal. Chem.*, vol. 592, no. 2, pp. 175–182, 2006, doi: 10.1016/j.jelechem.2006.05.010.

[10] Y. Yao, T. Zhou, C. Zhao, Q. Jing, and Y. Wang, “Influence of ZrO2 particles on fluorine-doped lead dioxide electrodeposition process from nitrate bath,” *Electrochim. Acta*, vol. 99, pp. 225–229, 2013, doi: 10.1016/j.electacta.2013.03.117.

[11] T. Mahalingam *et al.*, “Electrosynthesis and characterization of lead oxide thin films,” *Mater. Charact.*, vol. 58, no. 8-9 SPEC. ISS., pp. 817–822, 2007, doi: 10.1016/j.matchar.2006.11.021.

[12] U. Casellato, S. Cattarin, and M. Musiani, “Preparation of porous PbO2 electrodes by

electrochemical deposition of composites," *Electrochim. Acta*, vol. 48, no. 27, pp. 3991–3998, 2003, doi: 10.1016/S0013-4686(03)00527-9.

[13] A. B. Velichenko, D. V. Girenko, and F. I. Danilov, "Mechanism of lead dioxide electrodeposition," *J. Electroanal. Chem.*, vol. 405, no. 1–2, pp. 127–132, 1996, doi: 10.1016/0022-0728(95)04401-9.

[14] L. A. Yolshina, V. Y. Kudyakov, and V. G. Zyryanov, "Development of an electrode for lead-acid batteries possessing a high electrochemical utilization factor and invariable cycling characteristics," *J. Power Sources*, vol. 65, no. 1–2, pp. 71–76, 1997, doi: 10.1016/S0378-7753(97)02469-5.

[15] K. Ji, C. Xu, H. Zhao, and Z. Dai, "Electrodeposited lead-foam grids on copper-foam substrates as positive current collectors for lead-acid batteries," *J. Power Sources*, vol. 248, pp. 307–316, 2014, doi: 10.1016/j.jpowsour.2013.09.112.

[16] N. A. Hampson, "Carr, Hampson - 1972 - Lead dioxide electrode," vol. 157, no. 1971, 1972.

[17] P. Rüetschi, "Influence of Crystal Structure and Interparticle Contact on the Capacity of PbO2 Electrodes," *J. Electrochem. Soc.*, vol. 139, no. 5, pp. 1347–1351, 1992, doi: 10.1149/1.2069410.

[18] Y. Kim, "Information To Users Umi," *Dissertation*, p. 274, 2002.

[19] M. Cao, C. Hu, G. Peng, Y. Qi, and E. Wang, "Selected-control synthesis of PbO2 and Pb3O4 single-crystalline nanorods," *J. Am. Chem. Soc.*, vol. 125, no. 17, pp. 4982–4983, 2003, doi: 10.1021/ja029620l.

[20] G. Xi, Y. Peng, L. Xu, M. Zhang, W. Yu, and Y. Qian, "Selected-control synthesis of PbO2 submicrometer-sized hollow spheres and Pb3O4 microtubes," *Inorg. Chem. Commun.*, vol. 7, no. 5, pp. 607–610, 2004, doi: 10.1016/j.inoche.2004.03.001.

[21] M. D. Hossain *et al.*, "Effects of additives on the morphology and stability of PbO2 films electrodeposited on nickel substrate for light weight lead-acid battery application," *J. Energy Storage*, vol. 27, no. November 2019, 2020, doi: 10.1016/j.est.2019.101108.

[22] c and M. M. Avijit Biswal, a, b, c Bankim Chandra Tripathy, a, b Tondepu Subbaiah, a, b Danielle Meyrick, "Dual Effect of Anionic Surfactants in the Electrodeposited MnO 2 Trafficking Redox Ions for Energy Storage Dual Effect of Anionic Surfactants in the Electrodeposited MnO 2 Trafficking Redox Ions for Energy Storage," *J. ofThe Electrochem. Soc. 162 A30-A38*, vol.

162, pp. A30–A38, 2015, doi: 10.1149/2.0191501jes.

[23] D. R. P. Egan, C. T. J. Low, and F. C. Walsh, “Electrodeposited nanostructured lead dioxide as a thin film electrode for a lightweight lead-acid battery,” *J. Power Sources*, vol. 196, no. 13, pp. 5725–5730, 2011, doi: 10.1016/j.jpowsour.2011.01.008.

[24] M. Taguchi and H. Sugita, “Analysis for electrolytic oxidation and reduction of PbSO4/Pb electrode by electrochemical QCM technique,” *J. Power Sources*, vol. 109, no. 2, pp. 294–300, 2002, doi: 10.1016/S0378-7753(02)00056-3.

[25] S. Ghasemi, M. F. Mousavi, and M. Shamsipur, “Electrochemical deposition of lead dioxide in the presence of polyvinylpyrrolidone. A morphological study,” *Electrochim. Acta*, vol. 53, no. 2, pp. 459–467, 2007, doi: 10.1016/j.electacta.2007.06.068.

[26] É. C. G. Rufino, M. H. P. Santana, L. A. De Faria, and L. M. Da Silva, “Influence of lead dioxide electrodes morphology on kinetics and current efficiency of oxygen-ozone evolution reactions,” *Chem. Pap.*, vol. 64, no. 6, pp. 749–757, 2010, doi: 10.2478/s11696-010-0062-2.

[27] S. Ghasemi, M. F. Mousavi, H. Karami, M. Shamsipur, and S. H. Kazemi, “Energy storage capacity investigation of pulsed current formed nano-structured lead dioxide,” *Electrochim. Acta*, vol. 52, no. 4, pp. 1596–1602, 2006, doi: 10.1016/j.electacta.2006.02.068.

[28] T. Chen, H. Huang, H. Ma, and D. Kong, “Effects of surface morphology of nanostructured PbO2 thin films on their electrochemical properties,” *Electrochim. Acta*, vol. 88, pp. 79–85, 2013, doi: 10.1016/j.electacta.2012.10.009.

[29] N. Yu, L. Gao, S. Zhao, and Z. Wang, “Electrodeposited PbO2 thin film as positive electrode in PbO2/AC hybrid capacitor,” *Electrochim. Acta*, vol. 54, no. 14, pp. 3835–3841, 2009, doi: 10.1016/j.electacta.2009.01.086.

[30] W. Zhang, C. Q. Tu, Y. F. Chen, W. Y. Li, and G. Houlachi, “Cyclic Voltammetric Studies of the Behavior of Lead-Silver Anodes in Zinc Electrolytes,” vol. 22, no. June, pp. 1672–1679, 2013, doi: 10.1007/s11665-012-0456-0.

[31] M. Ueda, A. Watanabe, T. Kameyama, Y. Matsumoto, M. Sekimoto, and T. Shimamune, “Performance characteristics of a new type of lead dioxide-coated titanium anode,” *J. Appl. Electrochem.*, vol. 25, no. 9, pp. 817–822, 1995, doi: 10.1007/BF00233899.

[32] B. ming CHEN, Z. cheng GUO, X. wan YANG, and Y. dong CAO, “Morphology of alpha-lead dioxide electrodeposited on aluminum substrate electrode,” *Trans. Nonferrous Met. Soc.*

China (English Ed., vol. 20, no. 1, pp. 97–103, 2010, doi: 10.1016/S1003-6326(09)60103-5.

[33] Z. He, M. D. Hayat, S. Huang, X. Wang, and P. Cao, " Physicochemical Characterization of PbO 2 Coatings Electrosynthesized from a Methanesulfonate Electrolytic Solution ," *J. Electrochem. Soc.*, vol. 165, no. 14, pp. D670–D675, 2018, doi: 10.1149/2.0161814jes.

[34] P. Ruetschi, "Ruetschi1977," *J. Power Sources, 2 3*, vol. 2, no. 1977178, pp. 3–24, 1977.

[35] M. D. Hossain, C. M. Mustafa, and M. M. Islam, "Effect of deposition parameters on the morphology and electrochemical behavior of lead dioxide," *J. Electrochem. Sci. Technol.*, vol. 8, no. 3, pp. 197–205, 2017, doi: 10.5229/JECST.2017.8.3.197.

[36] C. A. Melendres and M. Pankuch, "On the composition of the passive film on nickel: a surface-enhanced Raman spectroelectrochemical study," *J. Electroanal. Chem.*, vol. 333, no. 1–2, pp. 103–113, 1992, doi: 10.1016/0022-0728(92)80384-G.

[37] M. R. F. Hurtado, P. T. A. Sumodjo, and A. V. Benedetti, "Electrochemical studies with a Cu-5wt.%Ni alloy in 0.5 M H2SO4," *Electrochim. Acta*, vol. 48, no. 19, pp. 2791–2798, 2003, doi: 10.1016/S0013-4686(03)00413-4.

[38] T. M. P. Nguyen, "Lead Acid Batteries in Extreme Conditions: Accelerated Charge, Maintaining the Charge With Imposed Low Current, Polarity Inversions Introducing Non-Conventional Charge Methods," *HAL, Arch. Ouvert.*, p. 175, 2009.

[39] B. CHEN, Z. GUO, H. HUANG, X. YANG, and Y. CAO, "Effect of the current density on electrodepositing alpha-lead dioxide coating on aluminum substrate," *Acta Metall. Sin. (English Lett.*, vol. 22, no. 5, pp. 373–382, 2009, doi: 10.1016/S1006-7191(08)60111-8.

[40] J. Kong, S. Shi, L. Kong, X. Zhu, and J. Ni, "Preparation and characterization of PbO2 electrodes doped with different rare earth oxides," *Electrochim. Acta*, vol. 53, no. 4, pp. 2048–2054, 2007, doi: 10.1016/j.electacta.2007.09.003.